

iREVIEWS

STATE-OF-THE-ART PAPERS

Intravascular Imaging of Coronary Calcification and its Clinical Implications



Gary S. Mintz, MD

ABSTRACT

Calcium impacts the natural history and treatment of coronary artery disease in many ways. Intravascular imaging studies, mostly intravascular ultrasound, but more recently studies using optical coherence tomography, have been instrumental in increasing our understanding of the relationship between calcium and coronary atherosclerosis, the predictors, the natural history of this relationship, and the impact on treatment. On one hand, stable coronary lesions are associated with more calcium than unstable lesions; and the amount of calcium may affect the success of percutaneous coronary intervention. On the other hand, calcium correlates with plaque burden; unstable lesions are associated with focal calcium deposits; and calcific nodules are one of the morphologies of vulnerable plaque. This review focuses on more than 20 years of intravascular imaging studies of the relationship between calcium and coronary atherosclerosis. (J Am Coll Cardiol Img 2015;8:461-71) © 2015 by the American College of Cardiology Foundation.

The extent of coronary artery calcium strongly correlates with the degree of atherosclerosis and, therefore, with the rate of future cardiac events. Coronary angiography has low-to-moderate sensitivity compared with grayscale intravascular ultrasound (IVUS) or optical coherence tomography (OCT), the gold standard for coronary calcium detection; but coronary angiography has a relatively high positive predictive value. Stable coronary lesions are associated with more calcium than unstable lesions, and the amount of calcium may affect the success of percutaneous coronary intervention. Unstable lesions are associated with focal calcium deposits that may be related to fibrous cap disruption, and calcific nodules are one of the morphologies of vulnerable plaque. Certain patient populations are at higher risk for greater amounts of coronary calcium. This review summarizes the data that has been acquired with intravascular imaging.

DETECTION AND QUANTIFICATION OF CALCIUM

IVUS. Calcium is a powerful reflector of ultrasound; little of the beam enters or even penetrates calcium so that calcium casts a shadow over deeper arterial structures. The IVUS signature of calcium is echodense (hyperechoic) plaque that is brighter than the reference adventitia with shadowing (**Figure 1**); however, dense fibrous tissue is also echodense and can sometimes cast a shadow. Calcium, but not dense fibrous tissue, produces reverberations, multiple reflections from oscillation of ultrasound between the transducer and calcium to cause concentric arcs at reproducible distances, especially after calcium is treated with rotational or orbital atherectomy (**Figure 2**). Hyperechoic plaque with shadowing is highly sensitive, whereas reverberations are highly specific (**1**). With the exception of microcalcifications, IVUS is sensitive and specific for detecting calcium

From the Cardiovascular Research Foundation, New York, New York. Dr. Mintz has received honoraria from Acist, Volcano, and Boston Scientific; fellowship support from Boston Scientific; and research support from Volcano, St. Jude, and InfraRedX.

Manuscript received November 26, 2014; revised manuscript received January 21, 2015, accepted February 12, 2015.

ABBREVIATIONS AND ACRONYMS

CKD = chronic kidney disease

CrCl = creatinine clearance

CTO = chronic total occlusion

DICOM = digital imaging and communications in medicine

IVUS = intravascular ultrasound

MI = myocardial infarction

OCT = optical coherence tomography

RF-IVUS = radiofrequency intravascular ultrasound

IVUS-VH = intravascular ultrasound-virtual histology

within a plaque. In 1 recent in vitro study, IVUS did not detect calcium in 14.8% of segments containing histopathologic calcium; reasons included microcalcium deposits (9.4%) and deep calcium hidden behind a large necrotic core that produced echo-attenuation (5.4%) (2). Although IVUS frequently shows a large block of calcium, pathologically this is an uncommon finding; instead, there are more often multiple smaller fragments of calcium that coalesce on IVUS imaging.

Calcium is assessed quantitatively with IVUS according to the arc (measured in degrees, using a protractor centered on the lumen) and length (using motorized transducer pullback). Semiquantitative grading classifies calcium as absent or subtending 1, 2, 3, or 4 quadrants. Calcium is described qualitatively according to its location: lesion versus reference and superficial (leading edge of acoustic shadowing within the most shallow 50% of the plaque and media thickness) versus deep (leading edge of acoustic shadowing within the deepest 50% of the plaque and media thickness). Because little of the ultrasound beam penetrates the calcium, only the leading edge of the calcific deposit is seen; and the apparent “thickness” of the calcium reflection in a grayscale IVUS image is a function of transducer saturation by the reflected ultrasound energy and not of anatomic thickness, although a volumetric “index” of calcium can be calculated by integrating the arc and length of calcium.

DICOM-based grayscale IVUS signal intensity analysis (Indec Medical Systems, Santa Clara, California) has been used to assess calcium. In an in vitro analysis, the sensitivity was 86.7%, the specificity was 93.3%, and the predictive accuracy was 92.3% for detecting calcium. However, it was unclear whether this approach adds to the visual assessment of calcification. In addition, the predictive accuracy behind calcium (in areas of shadowing) fell from 82.7% to only 53.3% (3).

RADIOFREQUENCY-IVUS. There are 3 radiofrequency (RF)-IVUS technologies. All 3 have been validated in vitro; and sensitivity, specificity, and predictive accuracy are high. However, each approach to tissue classification is very different; they should not be lumped together but should be considered distinct technologies; comparisons among them can yield discordant results; and only IVUS virtual histology (IVUS-VH) (Volcano Corporation, San Diego, California) is widely available (4).

IVUS-VH applies a mathematical autoregressive model to 8 amplitude or RF spectral parameters, and

a statistical classification tree sorts combinations of these parameters to create 4 plaque components that are then color coded as fibrous tissue (dark green), fibrofatty tissue (light green), necrotic core (red), and dense calcium (white) (Figure 3) (5). IVUS-VH detects calcium as part of a fibrocalcific plaque or in the setting of a necrotic core (calcified fibroatheroma) (6). There is ongoing controversy whether IVUS-VH can “see” behind calcium. If calcification is nonconfluent with gaps of approximately 100 μm (as is common), then there is some level of ultrasound energy that, depending on the density and thickness of the calcium, is greater than random noise in the majority such that IVUS-VH assessment of calcium thickness, area, and volume as well as the composition of plaque within shadowed areas may be possible. However, in individual cases, it difficult to predict whether there is a definable signal versus mostly noise; the current hardware and software do not make this distinction, and therefore, the accuracy of tissue classification should be assumed to be reduced in such areas (7).

Implanted stents have an appearance that can be misclassified by IVUS-VH as “calcium with or without necrotic core” (8). Finally, an automated computational system has been developed to assess the spatial distribution with regard to location within the plaque as well as the relationship to the plaque-lumen border of each IVUS-VH plaque component, including calcification (9).

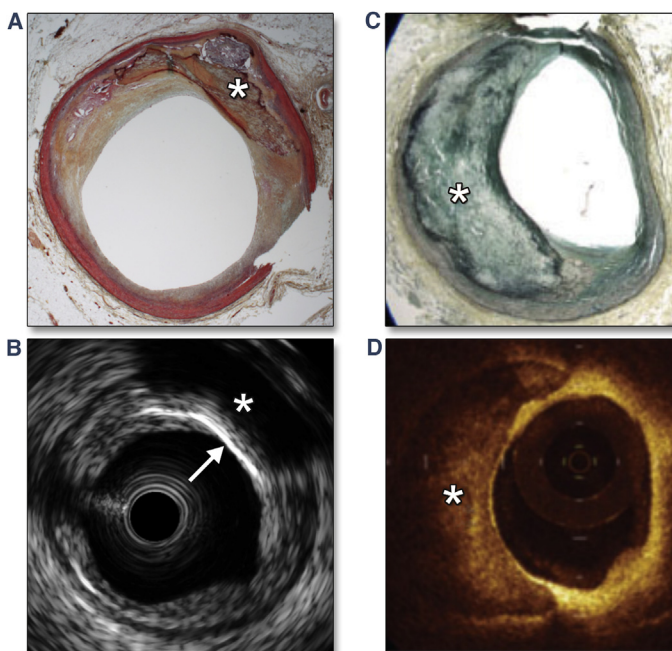
Integrated backscatter-IVUS (Visiwave, Terumo, Japan) uses just a single parameter, intensity of the backscatter or reflection of ultrasound, to assess plaque composition. There are significant differences in backscatter among: 1) thrombi; 2) fibrous tissue; 3) mixed lesions; 4) calcification; and 5) lipid core, intimal hyperplasia, and media that have similar values. Current systems color code tissue as red (calcium, -11 to -29 dB), dense fibrosis (yellow, -29 to -35 dB), green (fibrosis, -35 to -49 dB), and blue (lipid or intimal hyperplasia, -49 to -130 dB) (10).

iMAP (Boston Scientific, Fremont, California) is based on a mathematically defined measure of similarity comparing in vivo spectra versus a library of spectra that have been acquired in vitro and includes only regions with a high degree of confidence in matching geometry and well-defined tissue composition. iMAP also provides a measure of confidence for each region of interest. Although fibrous tissue is color coded light green, lipidic tissue is color coded yellow, necrotic core is color coded pink, and calcium is color coded blue, confidence regarding tissue classification is represented as transparency with high confidence characterizations shown with more opaque color (4).

OPTICAL COHERENCE TOMOGRAPHY. With optical coherence tomography (OCT) (St. Jude Medical, St. Paul, Minnesota and Terumo, Japan), calcium appears as a signal-poor or heterogeneous region with sharply delineated leading, trailing, and/or lateral borders (**Figure 1**). Unlike IVUS, where calcium is most often confused with dense fibrous tissue, OCT-detected calcium is most often confused with lipid or necrotic core; however, the signal-poor regions of calcium are sharply delineated whereas the signal-poor regions of lipid or a necrotic core have poorly defined or diffuse borders (11). Also unlike IVUS, penetration of calcium by OCT is greater than for other tissue types. Therefore, unlike IVUS, OCT can measure calcium thickness, area, and volume, and automatic quantification of these parameters may be possible (12).

CORONARY ANGIOGRAPHY. Angiographic calcium is classified as none or mild, moderate, or severe. Moderate calcification is defined as radiopacities noted only during the cardiac cycle before contrast injection, whereas severe calcification is defined as radiopacities seen without cardiac motion, usually affecting both sides of the arterial lumen. In the largest study of 1,155 target lesions ($n = 1,117$), 73% contained grayscale IVUS calcium: 26% were 1-quadrant, 21% were 2-quadrant, 15% were 3-quadrant, and 11% were 4-quadrant calcium. Of these, only 26% had moderate angiographic calcium, and 12% had severe angiographic calcium. The overall sensitivity of angiography was 48%, lowest in lesions with 1-quadrant calcium and highest (85%) in lesions with 4-quadrant calcium. In this study, coronary angiography detected superficial target lesion calcium, either alone or in combination with deep calcium, more often than isolated deep calcium presumably because superficial calcium was presumably thicker than deep calcium, potentially occupying full plaque thickness. The overall angiographic specificity was 89%, highest (98%) for angiographic severe calcium (**Table 1**). However, the angiographic false-positive rate of 11% could not be explained, even by the presence of isolated reference segment calcification (13). In a study by Tuzcu et al. (14) in 183 patients, the only angiographic predictor of grayscale IVUS-detected calcium was angiographic calcification elsewhere in the coronary tree. However, it must be noted that both of these studies were published approximately 20 years ago, and there have been significant improvements in angiographic equipment since then. Finally, in a study of 67 chronic total occlusions (CTO), IVUS detected calcium in 96% of occlusions whereas angiography detected calcium in 61% (15).

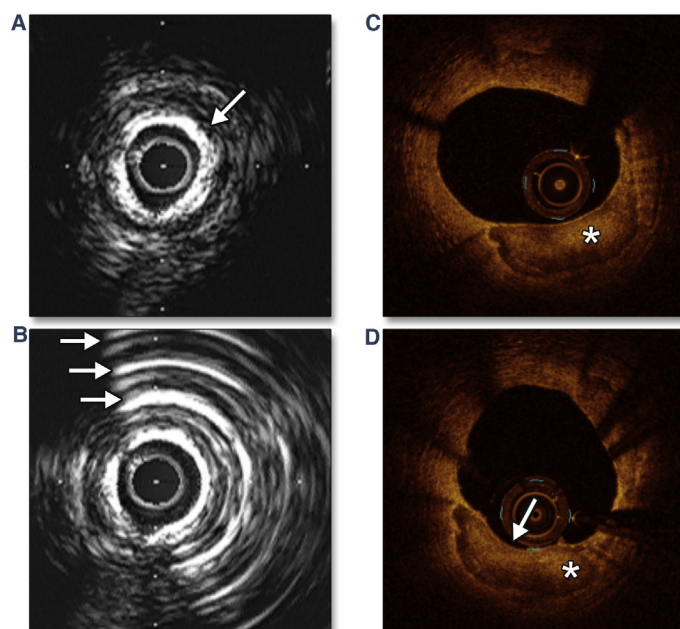
FIGURE 1 IVUS and OCT Images of Coronary Artery Calcium



(**A and B**) Comparison of histopathology and IVUS images of coronary calcium. On the IVUS image note the bright leading edge of superficial calcium (brighter than the adventitia and closer to the lumen than to the adventitia) (**B**, white arrow) with deeper shadowing (**B**, white asterisk) that corresponds to the histopathological calcium (white asterisk). Calcium thickness and area cannot be assessed. (**C and D**) Comparison of histopathology and OCT images of coronary calcium (**D**, white asterisk). On the OCT image, note the signal-poor and heterogeneous region with sharply delineated leading, trailing, and lateral borders. Calcium thickness and area can be measured. (**A and B**) Reprinted with permission from Lee et al. (51). (**C and D**) From Coletta J, Suzuki N, Nascimento BR, et al. Uso da tomografia de coerência óptica intracoronariana para caracterização precisa da aterosclerose. Arquivos Brasileiros de Cardiologia 2010;94:268-272. IVUS = intravascular ultrasound; OCT = optical coherence tomography.

COMPUTED TOMOGRAPHY. A coronary calcium score is calculated using a weighted value assigned to the highest density of calcification in each coronary segment that is then multiplied by the area and finally summed for all arteries to give a total coronary artery calcium score that has been correlated with patient outcomes (16). Three in vivo and 1 in vitro grayscale IVUS study have suggested that the amount of coronary artery calcium correlates with coronary artery plaque burden (17-20) and that plaque burden predicts outcomes (21). More recently, albeit in relatively small numbers of patients, lesion-specific parameters on multidetector imaging such as spotty calcium have been correlated with similar VH and grayscale IVUS findings that are indicative of unstable plaques (22-26).

FIGURE 2 IVUS and OCT Examples After Rotational Atherectomy and Orbital Atherectomy



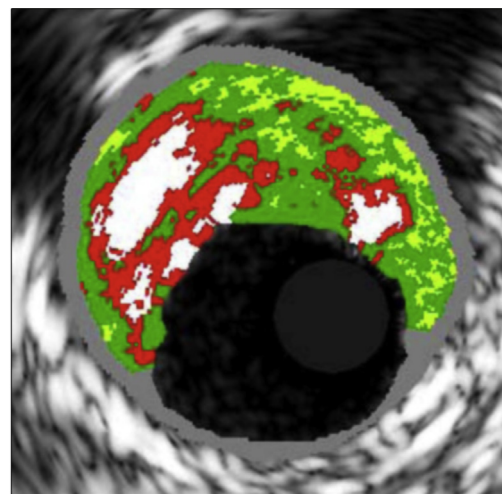
(A and B) IVUS images before and after rotational atherectomy, respectively. Note the near circumferential superficial calcium pre-intervention (A, white arrow) and the development of multiple reverberations after rotational atherectomy (B, white arrows). (C and D) OCT images before and after orbital atherectomy, respectively. Note the larger deposit of calcium (C, white asterisk), whose thickness is reduced by orbital atherectomy (D, white arrow). Abbreviations as in Figure 1.

ANATOMIC AND CLINICAL FACTORS ASSOCIATED WITH CALCIFICATION AND ITS DEVELOPMENT

ANATOMIC FACTORS. Grayscale IVUS detected more calcium in lesions than in reference segments, in severe stenoses than in mild stenoses, in CTOs than in severe stenoses, in negative remodeling than in positive remodeling in patients with stable angina, and in smaller than in larger vessels (15,17,27-30). Almost all CTOs have some calcium, albeit sometimes only in small amounts (15,28). Several studies have reported increasing amounts grayscale IVUS-detected calcium in relationship to increasing plaque burden, perhaps explaining the utility of the CT calcium score to predict clinical events (17,18).

After primary stent implantation, calcium can evolve from attenuated plaque (the most predictive grayscale IVUS feature of a fibroatheroma) (31). Calcification can also occur in association with a necrotic core (as part of a calcified fibroatheroma) (6)

FIGURE 3 Typical IVUS-VH Image



IVUS-VH is one IVUS technology incorporating radiofrequency data to assess plaque composition. Fibrous tissue is dark green, fibrofatty tissue is light green, necrotic core is red, and dense calcium is white. IVUS-VH = intravascular ultrasound-virtual histology.

and can be seen within in-stent neoatherosclerosis (32-34).

Calcium is not limited to native coronary arteries but can also occur in saphenous vein grafts, albeit less commonly than in native arteries. In a grayscale IVUS study of 334 vein grafts in 274 consecutive patients, calcium was found in 133 patients (40%), especially in older vein grafts (35).

Clinical factors include increasing patient age, male versus female sex, hypertension, non-insulin-treated diabetes, stable (vs. unstable) angina (17,30,36-39), and renal function, especially the need for or transition to hemodialysis, are predictors of the presence and amount of lesion-associated calcium as assessed by grayscale or IVUS-VH or OCT. Gruberg et al. (40) reported 142 patients who underwent pre-intervention grayscale IVUS imaging of a de novo native coronary artery stenosis before percutaneous intervention and who were grouped according to calculated creatinine clearance (CrCl) concentration of >70 ml/min, 50 to 69 ml/min, <50 ml/min, and end-stage renal disease. No significant differences were found in any of the IVUS measurements among patients with CrCl of >70, 50 to 69, and <50 ml/min; conversely, patients with end-stage renal disease had larger arcs of calcium (40). In an OCT study by Kato et al. (41), 61 plaques from 37 patients with

chronic kidney disease (CKD) (defined as estimated glomerular filtration rate of <60 ml/min per 1.73 m²) had more calcification than 402 plaques in 250 patients without CKD. In the PROSPECT (Providing Regional Observations to Study Predictors of Events in the Coronary Tree) study, 280 nonculprit lesions in patients with CKD had a greater percentage of IVUS-VH dense calcium than 2,390 non-culprit lesions in patients without CKD (42). Finally, in 78 patients with CKD divided into 4 groups based on their estimated glomerular filtration rate, IVUS-VH showed an increase in the relative volume of dense calcium with decreasing renal function that was most significant in patients undergoing hemodialysis (43).

In addition to graft age, insulin-treated diabetes mellitus and tobacco use predicted the development of grayscale IVUS saphenous vein graft calcification (34). Bypass surgery to the left coronary system appears to increase calcification and negative remodeling of the “upstream” left main coronary artery (44).

UNSTABLE CORONARY ARTERY DISEASE

Although both classic and recent grayscale and IVUS-VH studies comparing stable versus unstable lesions have indicated that stable lesions have more extensive calcium than unstable lesions, other studies have suggested that the relationship between calcium and lesion stability is more complicated (36-38,45-47).

SPOTTY CALCIUM. In 2004, Ehara et al. (38) reported that the frequency and number of grayscale IVUS-detected culprit lesion calcium deposits with an arc of <90° (i.e., spotty calcium) were significantly greater in patients with an acute myocardial infarction (MI) than in patients with stable or unstable angina. This was confirmed in a grayscale IVUS study by Fujii et al. (45) and in an OCT study performed by Mizukoshi et al. (47) in which the arc, area, and length of calcium were significantly smaller and the number of large calcium deposits was significantly less in patients with acute MI or unstable angina than in patients with stable angina. Conversely, the prevalence of spotty calcium deposits was significantly greater in acute MI or unstable angina, and there was a relationship between plaque rupture and the number of spotty calcium deposits (47). Histopathology studies have suggested that symptomatic plaque ruptures are superimposed on previously asymptomatic and healed plaque rupture sites (48). IVUS or OCT spotty calcium deposits within unstable lesions may represent in vivo “footprints” of these old ruptures that subsequently healed. In support of this, Pu et al. (2) assessed unstable lesion morphology including spotty calcification in 2,294 vessel

TABLE 1 Comparison of Angiographic and IVUS-Detected Coronary Calcification*

IVUS	Angiographic Calcification		
	None or Mild	Moderate†	Severe†
No. of lesions	715	306	134
Percentage of target lesion calcium	61%	90%	98%
Arc of lesion calcium	71° ± 83°	165° ± 106°	238° ± 104°
Percentage of superficial lesion calcium	37%	72%	92%
Arc of superficial lesion calcium	44° ± 74°	124° ± 110°	215° ± 119°
Arc of reference calcium, °	25° ± 63°	61° ± 93°	87° ± 98°
Total length of calcium, mm	3.6 ± 4.4	7.2 ± 6.4	9.7 ± 6.4

*Table data from Mintz et al. (13). †Moderate calcification = radiopacities are noted only during the cardiac cycle before contrast injection; severe calcification = radiopacities are seen without cardiac motion, also before contrast injection, usually affecting both sides of the arterial lumen.

IVUS = intravascular ultrasound.

segments from 151 coronary specimens from 62 patients. In 14.4% of segments, there was grayscale IVUS-detected spotty calcification; 62.4% were fibroatheromas with calcium deposits, and 32.7% were fibrocalcific plaques. When histological results were considered, the standard, grayscale IVUS spotty calcification had a sensitivity of 69.4% and a specificity of 71.7% for the detection of a fibroatheroma with calcium deposits. When classified by location, 72.6% of IVUS superficial spotty calcifications were seen in a fibroatheroma with calcium deposits (45.3% late and 27.3% early necrotic core). Conversely, most deep spotty calcifications (67.4%) were seen in fibrocalcific plaques without a necrotic while only 32.6% of deep spotty calcifications were seen in fibroatheromas. IVUS spotty calcification was also associated with near infrared spectroscopy-detected lipid-rich plaque. Finally, spotty calcification has also been associated with more extensive and diffuse coronary atherosclerosis and accelerated disease progression (49).

CALCIFIED NODULE. In the first clinical report in 1996, Dussaillant et al. (50) presented 3 patients with classic angiographic features of an intracoronary thrombus, but in whom grayscale IVUS showed “that the filling defects were not thrombi, but calcified (presumably atherosclerotic) masses.” Subsequently in an in vitro validation study, IVUS characteristics of a calcified nodule were shown to be: 1) a convex shape of the luminal surface (94.1% of calcified nodules vs. 9.7% of non-nodular calcium); 2) a convex shape of the luminal side of calcium (100% vs. 16.0%); 3) an irregular luminal surface (64.7% vs. 11.6%); and 4) an irregular leading edge of calcium (88.2% vs. 19.0%) (51). In a pre-intervention culprit lesion OCT analysis of 126 patients with an acute coronary syndrome, Jia et al. (52) reported a 43.7% prevalence of plaque rupture, a 31.0% prevalence of plaque erosion,

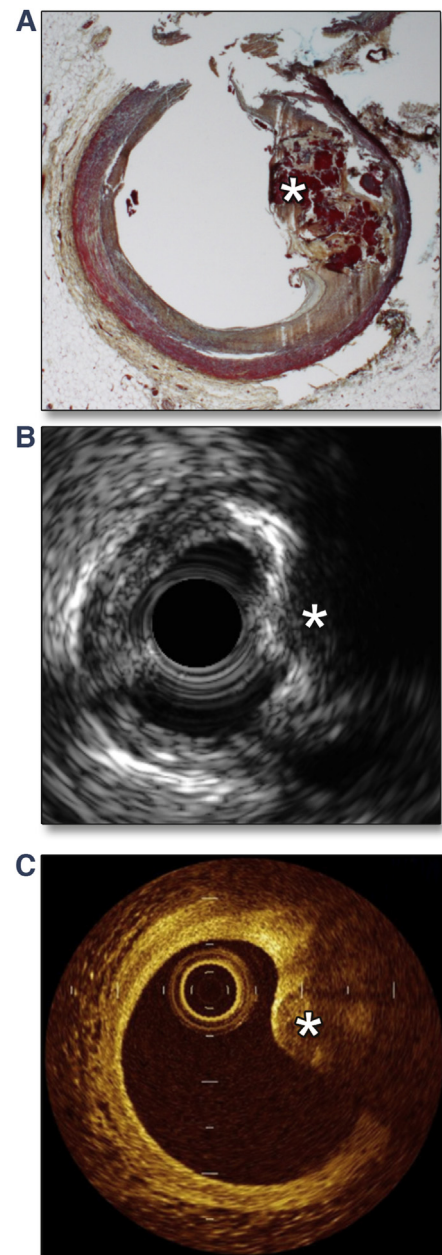
and a 7.9% prevalence of calcified nodule. Calcified nodules were seen in the oldest patients, who most often presented with non-ST-segment elevation MI and white rather than red thrombi. Finally, from the 3-vessel grayscale and IVUS-VH PROSPECT (Providing Regional Observations to Study Predictors of Events in the Coronary Tree) study, Xu et al. (53) reported 314 secondary, nonculprit calcified nodules in 1,573 arteries in 623 patients. The axial locations of these calcified nodules were similar to those in previous reports of fibroatheromas or plaque ruptures assessed by IVUS-VH, OCT, or histopathology or acute coronary thrombosis assessed angiographically (54-58). Although secondary calcified nodules were more common in older individuals, they were (surprisingly) associated with fewer (not more) events during 3-year follow-up (53). Examples are shown in Figure 4.

MICROCALCIFICATIONS. It has been suggested that microcalcifications ($>5\ \mu\text{m}$) in fibrous caps of fibroatheromas can increase local tissue stress by a factor of at least 2 (surpassing the ultimate stress threshold for fibrous cap rupture) to promote cavitation-induced plaque rupture, depending on their size, distribution, orientation, and aspect ratio (59). A theoretical model predicts that cap rupture can occur in the center of a fibrous cap whose thickness is $<65\ \mu\text{m}$, in close agreement with histopathology observations (60,61). Conversely, cell-level calcifications contained within the necrotic core are not high risk from a mechanical standpoint because they reside within a viscous lipid pool that does not support significant tensile stress, the exact opposite of microcalcification in the fibrous cap, although they may coalesce as part of a calcified fibroatheroma or to form a calcific nodule. Current OCT technology has the highest resolution of any intracoronary imaging modality, but even the resolution of OCT is too coarse for visualizing microcalcification. A new form of OCT, termed micro-OCT, has been developed with a resolution that is improved by an order of magnitude compared to conventional OCT (62).

IMPACT OF CALCIFICATION ON PERCUTANEOUS CORONARY INTERVENTION

Clinical experience has shown that severe calcification as assessed by intravascular imaging limits stent expansion and that severe stent underexpansion can be associated with adverse events including restenosis and stent thrombosis (63). Treating stent underexpansion in a heavily calcified lesion is more difficult than preventing underexpansion (64). However, there is a lack of systematic, consistent, conclusive confirmatory data with any intravascular

FIGURE 4 IVUS and OCT Images of a Calcified Coronary Nodule



(A and B) Comparison of histopathology and IVUS images of a calcified coronary nodule (A, asterisk). The IVUS image shows the convex shape of the luminal surface and luminal side of calcium and the irregular luminal surface and leading edge of calcium (compare this to the non-nodular calcium shown in Figures 1B, 2A, and 2B). (C) OCT image shows protrusion of a signal-poor or heterogeneous region with a sharply delineated border (i.e., calcium) into the lumen (compare this scan to those in Figures 1D, 2C, and 2D). Abbreviations as in Figure 1. (A and B) Reprinted with permission from Lee et al. (51). (C) Reprinted with permission from Kubo et al. (93).

imaging technique (grayscale IVUS, RF-IVUS, or OCT) in a large numbers of patients, in part because severely calcified lesions are not very common, can be hard to cross and image pre-intervention; and when recognized angiographically are often treated with plaque modification devices (excimer laser angioplasty, rotational or orbital atherectomy, or cutting or scoring balloon atherectomy) before stent implantation and/or high-pressure adjunctive balloon inflations after stent implantation (65-69). Similarly, although there is general agreement that the greater the arc, length, or thickness of calcium, the greater is the likelihood of stent underexpansion, there are no published cutoffs that can be used as guidelines for recommending lesion modification prior to stent implantation or the need for high-pressure adjunctive balloon inflations afterward. On the other hand, iterative intravascular imaging in conjunction with repeated high-pressure adjunctive balloon inflations can be used to optimize stent expansion (and treat post-procedure stent underexpansion) in a way not possible using angiography alone.

Lesion preparation can involve the use of a cutting or scoring balloon, excimer laser angioplasty, or rotational or orbital atherectomy. Sequential grayscale IVUS and OCT studies have shown that excimer laser coronary angioplasty does not decrease lesion-associated calcium but causes dissections and, especially, fragmentation of calcific deposits, presumably as part of its photoacoustic effect (70,71). Grayscale IVUS and OCT studies have shown that rotational (and probably) orbital atherectomy ablate calcium to cause fissuring or cracks within the ablated calcium (72,73). Calcium limits vessel expansion and impacts the mechanism of balloon dilation, either as a stand-alone technique, after excimer laser angioplasty or rotational atherectomy, or after stent implantation (70,72-74).

One recent study suggests that calcium at the ostium of the left circumflex is associated with narrowing of the ostium of the left circumflex after crossover stenting from the left main to the left anterior descending coronary artery (75).

COMPLICATIONS. Greater amounts of IVUS-detected lesion calcification have been associated with percutaneous intervention procedural enzyme elevation; however, this may have been influenced by greater use of rotational atherectomy in calcified lesions in these studies (76,77). OCT-detected spotty calcification is also associated with periprocedural enzyme elevation, especially when colocalized to an OCT-detected thin cap fibroatheroma; this is consistent with findings of similarly unstable culprit lesion

morphology in acute coronary syndrome patients and other studies suggesting that “vulnerable plaques” are not only prone to rupture but can cause periprocedural MI (2,45,78,79). Conversely, post-stent plaque prolapse is less apparent in calcified than in non-calcified lesions such as thrombus-containing lesions, thin-cap fibroatheromas, or lesions containing lipid-rich plaque (80). When CTOs are treated, intramural hematomas and post-procedure Thrombolysis In Myocardial Infarction (TIMI) flow grade <3 are seen in CTO lesions with greater amounts of calcium (15).

Grayscale IVUS studies have shown that localized calcium deposits or the transition from calcified to noncalcified plaque (or to normal vessel wall) are foci for balloon dilation-associated dissection; and more extensive dissections occur in segments of the arteries that are more heavily calcified (81-83). Conversely, calcification limits the axial propagation of an intramural hematoma that tends to occur most often at edges of stents implanted into nondiseased reference segments (83,84).

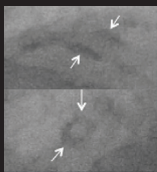
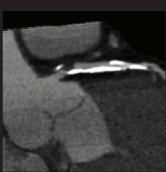
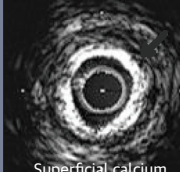
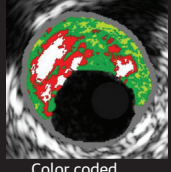

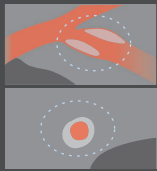
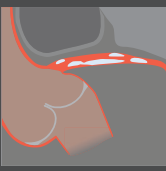
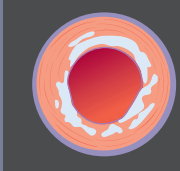
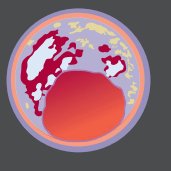
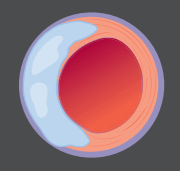
Grayscale IVUS and OCT studies have shown that severe calcification is associated with more acute malapposition, and OCT also has shown that acute malapposition is affected by the circumferential arc of calcium, rather than its depth (77,85). Although stent implantation into calcified lesions is more often associated with stent fracture (86), calcium does not appear to be otherwise associated with increased amounts of intimal hyperplasia at follow-up, especially after drug-eluting stent implantation (87,88).

PROGRESSION AND REGRESSION

Assessing quantitative changes in coronary atherosclerosis using grayscale IVUS or plaque composition with RF-IVUS or OCT has been increasingly used in clinical trials of progression and regression. However, because calcium is a strong reflector of ultrasound so that deeper arterial structures including the atherosclerotic plaque are shadowed, calcification affects the analysis of plaque volume and plaque burden. Although from a practical standpoint, patients enrolled in progression/regression studies do not have severe calcification, calcium tends to be one of the leading reasons for exclusion of patients from such studies.

In a grayscale IVUS analysis of 776 patients from REVERSAL (Reversal of Atherosclerosis With Aggressive Lipid Lowering) and CAMELOT (Comparison of Amlodipine Versus Enalapril to Limit Occurrences of Thrombosis), Nicholls et al. (30) showed that

CENTRAL ILLUSTRATION Detection, Localization, and Quantification of Coronary Calcium by Various Imaging Modalities

	Coronary Angiography	CT	IVUS	RF-IVUS (IVUS-VH)	OCT
IMAGING MODALITIES			 Superficial calcium detection	 Color coded tissue composition	 Sharp delineation of calcium area is possible
Detection of coronary artery calcium	+	+++	+++	+++	++++
Localization of coronary artery calcium	+	+++	+++	+++	++++
Quantification of coronary artery calcium	+	+++	++	+++	++++
					

Coronary angiography, coronary computed tomography (CT), intravascular ultrasound (IVUS), radiofrequency (RF) intravascular ultrasound-virtual histology (IVUS-VH), and optical coherence tomography (OCT) can all detect and attempt to localize and quantify calcium, albeit with very different diagnostic accuracies.

plaques with more calcium were more resistant to change than plaques with less calcium which were more likely to undergo either progression or regression in response to pharmacologic interventions. Using the data from SATURN (Study of Coronary Atheroma by Intravascular Ultrasound: Effect of rosuvastatin versus atorvastatin) in a IVUS-VH analysis, these same authors showed an increase in dense calcium volume in 71 patients treated with high-dose rosuvastatin or atorvastatin for 24 months (89). There was a similar finding in a IVUS-VH analysis of 99 nonculprit lesions in 63 ST-segment elevation MI patients imaged in the HORIZONS-AMI (Harmonizing Outcomes with Revascularization and Stents in Acute Myocardial Infarction) trial, in keeping with the evolution of attenuated plaque to calcified plaque after stent implantation into

culprit lesions, as was also reported in HORIZONS-AMI study (31,90).

In support of these serial studies, 2 studies using IVUS-VH showed that nontreated, fibrocalcific lesions did not progress (there were no changes in lumen dimensions or plaque burden) during a 12-month observational period and that nonculprit fibrocalcific lesions were associated with a lack of adverse events during a 3-year follow-up period (91,92).

CONCLUSIONS

Calcium impacts the natural history and treatment of coronary artery disease in many ways. Intravascular imaging studies, especially IVUS over the last 20 or more years, have been instrumental in

understanding the relationship between calcium and coronary atherosclerosis. The **Central Illustration** summarizes the various clinical modalities that are available to detect, localize, and quantify coronary artery calcium.

REPRINT REQUESTS AND CORRESPONDENCE: Dr.

Gary S. Mintz, Cardiovascular Research Foundation, 111 East 59th Street, 11th Floor, New York, New York 10022. E-mail: gmintz@crf.org.

REFERENCES

1. Mintz GS, Nissen SE, Anderson WD, et al. Standards for the acquisition, measurement, and reporting of intravascular ultrasound studies: a report of the American College of Cardiology Task Force on Clinical Expert Consensus Documents. *J Am Coll Cardiol* 2001;37:1478-92.
2. Pu J, Mintz GS, Biro S, et al. Insights into echo-attenuated plaques, echolucent plaques, and plaques with spotty calcification: novel findings from comparisons among intravascular ultrasound, near-infrared spectroscopy, and pathological histology in 2,294 human coronary artery segments. *J Am Coll Cardiol* 2014;63:2220-33.
3. Kim SW, Mintz GS, Lee WS, et al. DICOM-based intravascular ultrasound signal intensity analysis: an Echoplague Medical Imaging Bench study. *Coron Artery Dis* 2014;25:236-41.
4. García-García HM, Gogas BD, Serruys PW, Bruining N. IVUS-based imaging modalities for tissue characterization: similarities and differences. *Int J Cardiovasc Imaging* 2011;27:215-24.
5. Nair A, Margolis MP, Kuban BD, Vince DG. Automated coronary plaque characterisation with intravascular ultrasound backscatter: ex vivo validation. *Eurointervention* 2007;3:113-20.
6. García-García HM, Mintz GS, Lerman A, et al. Tissue characterisation using intravascular radio-frequency data analysis: recommendations for acquisition, analysis, interpretation and reporting. *Eurointervention* 2009;5:177-89.
7. Pu J, Mintz GS, Brilakis ES, et al. In vivo characterization of coronary plaques: novel findings from comparing greyscale and virtual histology intravascular ultrasound and near-infrared spectroscopy. *Eur Heart J* 2012;33:372-83.
8. Kim SW, Mintz GS, Hong YJ, et al. The virtual histology intravascular ultrasound appearance of newly placed drug-eluting stents. *Am J Cardiol* 2008;102:1182-6.
9. Papaioannou TG, Schizas D, Vavuranakis M, Katsarou O, Soulis D, Stefanadis C. Quantification of new structural features of coronary plaques by computational post-hoc analysis of virtual histology-intravascular ultrasound images. *Comput Methods Biomech Biomed Engin* 2014;17:643-51.
10. Ohota M, Kawasaki M, Ismail TF, Hattori K, Serruys PW, Ozaki Y. A histological and clinical comparison of new and conventional integrated backscatter intravascular ultrasound (IB-IVUS). *Circ J* 2012;76:1678-86.
11. Tearney GJ, Regar E, Akasaka T, et al. International Working Group for Intravascular Optical Coherence Tomography (IWG-IVOC). Consensus standards for acquisition, measurement, and reporting of intravascular optical coherence tomography studies: a report from the International Working Group for Intravascular Optical Coherence Tomography Standardization and Validation. *J Am Coll Cardiol* 2012;59:1058-72.
12. Mehanna E, Bezerra HG, Prabhu D, et al. Volumetric characterization of human coronary calcification by frequency-domain optical coherence tomography. *Circ J* 2013;77:2334-40.
13. Mintz GS, Popma JJ, Pichard AD, et al. Patterns of calcification in coronary artery disease. A statistical analysis of intravascular ultrasound and coronary angiography in 1155 lesions. *Circulation* 1995;91:1959-65.
14. Tuzcu EM, Berkalp B, De Franco AC, et al. The dilemma of diagnosing coronary calcification: angiography versus intravascular ultrasound. *J Am Coll Cardiol* 1996;27:832-8.
15. Fujii K, Ochiai M, Mintz GS, et al. Procedural implications of intravascular ultrasound morphologic features of chronic total coronary occlusions. *Am J Cardiol* 2006;97:1455-62.
16. Youssef G, Kalia N, Darabian S, Budoff MJ. Coronary calcium: new insights, recent data, and clinical role. *Curr Cardiol Rep* 2013;15:325.
17. Mintz GS, Pichard AD, Popma JJ, et al. Determinants and correlates of target lesion calcium in coronary artery disease: a clinical, angiographic and intravascular ultrasound study. *J Am Coll Cardiol* 1997;29:268-74.
18. Tinana A, Mintz GS, Weissman NJ. Volumetric intravascular ultrasound quantification of the amount of atherosclerosis and calcium in non-stenotic arterial segments. *Am J Cardiol* 2002;89:757-60.
19. Qian J, Maehara A, Mintz GS, et al. Relation between individual plaque components and overall plaque burden in the prospective, multicenter virtual histology intravascular ultrasound registry. *Am J Cardiol* 2009;104:501-6.
20. Sangiorgi G, Rumberger JA, Severson A, et al. Arterial calcification and not lumen stenosis is highly correlated with atherosclerotic plaque burden in humans: a histologic study of 723 coronary artery segments using nondecalcifying methodology. *J Am Coll Cardiol* 1998;31:126-33.
21. Nicholls SJ, Hsu A, Wolski K, et al. Intravascular ultrasound-derived measures of coronary atherosclerotic plaque burden and clinical outcome. *J Am Coll Cardiol* 2010;55:2399-407.
22. Funada R, Oikawa Y, Yajima J, et al. The potential of RF backscattered IVUS data and multidetector-row computed tomography images for tissue characterization of human coronary atherosclerotic plaques. *Int J Cardiovasc Imaging* 2009;25:471-8.
23. Choi YH, Hong YJ, Park IH, et al. Relationship between coronary artery calcium score by multi-detector computed tomography and plaque components by virtual histology intravascular ultrasound. *J Korean Med Sci* 2011;26:1052-60.
24. van Velzen JE, de Graaf FR, Jukema JW, et al. Comparison of the relation between the calcium score and plaque characteristics in patients with acute coronary syndrome versus patients with stable coronary artery disease, assessed by computed tomography angiography and virtual histology intravascular ultrasound. *Am J Cardiol* 2011;108:658-64.
25. Kim SY, Kim KS, Seung MJ, et al. The culprit lesion score on multi-detector computed tomography can detect vulnerable coronary artery plaque. *Int J Cardiovasc Imaging* 2010;26 Suppl 2: 245-52.
26. de Graaf MA, Broersen A, Kitslaar PH, et al. Automatic quantification and characterization of coronary atherosclerosis with computed tomography coronary angiography: cross-correlation with intravascular ultrasound virtual histology. *Int J Cardiovasc Imaging* 2013;29:177-90.
27. Mintz GS, Pichard AD, Kent KM, Satler LF, Popma JJ, Leon MB. Interrelation of coronary angiographic reference lumen size and intravascular ultrasound target lesion calcium. *Am J Cardiol* 1998;81:387-91.
28. Guo J, Maehara A, Guo N, et al. Virtual histology intravascular ultrasound comparison of coronary chronic total occlusions versus non-occlusive lesions. *Int J Cardiovasc Imaging* 2013; 29:1249-54.
29. Mintz GS, Kent KM, Pichard AD, Satler LF, Popma JJ, Leon MB. Contribution of inadequate arterial remodeling to the development of focal coronary artery stenoses. An intravascular ultrasound study. *Circulation* 1997;95:1791-8.
30. Nicholls SJ, Tuzcu EM, Wolski K, et al. Coronary artery calcification and changes in atheroma burden in response to established medical therapies. *J Am Coll Cardiol* 2007;49:263-70.
31. Xu K, Mintz GS, Kubo T, et al. Long-term follow-up of attenuated plaques in patients with acute myocardial infarction: an intravascular ultrasound substudy of the HORIZONS-AMI trial. *Circ Cardiovasc Interv* 2012;5:185-92.
32. Hakim DA, Mintz GS, Sanidas E, et al. Serial gray scale intravascular ultrasound findings in late drug-eluting stent restenosis. *Am J Cardiol* 2013; 111:695-9.

33. Kang SJ, Mintz GS, Park DW, et al. Tissue characterization of in-stent neointima using intravascular ultrasound radiofrequency data analysis. *Am J Cardiol* 2010;106:1561-5.
34. Kang SJ, Mintz GS, Park DW, et al. Optical coherence tomographic analysis of in-stent neointima after drug-eluting stent implantation. *Circulation* 2011;123:2954-63.
35. Castagna MT, Mintz GS, Ohlmann P, et al. Incidence, location, magnitude, and clinical correlates of saphenous vein graft calcification: an intravascular ultrasound and angiographic study. *Circulation* 2005;111:1148-52.
36. Rasheed Q, Nair RN, Sheehan HM, Hodgson JM. Coronary artery plaque morphology in stable angina and subsets of unstable angina: an in vivo intracoronary ultrasound study. *Int J Card Imaging* 1995;11:89-95.
37. Nakamura M, Nishikawa H, Mukai S, et al. Impact of coronary artery remodeling on clinical presentation of coronary artery disease: an intravascular ultrasound study. *J Am Coll Cardiol* 2001;37:63-9.
38. Ehara S, Kobayashi Y, Yoshiyama M, et al. Spotty calcification typifies the culprit plaque in patients with acute myocardial infarction: an intravascular ultrasound study. *Circulation* 2004;110:3424-9.
39. Lansky AJ, Ng VG, Maehara A, et al. Gender and the extent of coronary atherosclerosis, plaque composition, and clinical outcomes in acute coronary syndromes. *J Am Coll Cardiol* 2012;59:562-72.
40. Gruberg L, Rai P, Mintz GS, et al. Impact of renal function on coronary plaque morphology and morphometry in patients with chronic renal insufficiency as determined by intravascular ultrasound volumetric analysis. *Am J Cardiol* 2005;96:892-6.
41. Kato K, Yonetsu T, Jia H, et al. Nonculprit coronary plaque characteristics of chronic kidney disease. *Circ Cardiovasc Imaging* 2013;6:448-56.
42. Baber U, Stone GW, Weisz G, et al. Coronary plaque composition, morphology, and outcomes in patients with and without chronic kidney disease presenting with acute coronary syndromes. *J Am Coll Cardiol* 2012;59:553-61.
43. Kono K, Fujii H, Nakai K, et al. Composition and plaque patterns of coronary culprit lesions and clinical characteristics of patients with chronic kidney disease. *Kidney Int* 2012;82:344-51.
44. Shang Y, Mintz GS, Pu J, et al. Bypass to the left coronary artery system may accelerate left main coronary artery negative remodeling and calcification. *Clin Res Cardiol* 2013;102:831-5.
45. Fujii K, Carlier SG, Mintz GS, et al. Intravascular ultrasound study of patterns of calcium in ruptured coronary plaques. *Am J Cardiol* 2005;96:352-7.
46. Vazquez-Figueroa JG, Rinehart S, Qian Z, et al. Prospective validation that vulnerable plaque associated with major adverse outcomes have larger plaque volume, less dense calcium, and more non-calcified plaque by quantitative, three-dimensional measurements using intravascular ultrasound with radiofrequency backscatter analysis: results from the ATLANTA I study. *J Cardiovasc Transl Res* 2013;6:762-71.
47. Mizukoshi M, Kubo T, Takarada S, et al. Coronary superficial and spotty calcium deposits in culprit coronary lesions of acute coronary syndrome as determined by optical coherence tomography. *Am J Cardiol* 2013;112:34-40.
48. Burke AP, Kolodgie FD, Farb A, et al. Healed plaque ruptures and sudden coronary death: evidence that subclinical rupture has a role in plaque progression. *Circulation* 2001;103:934-40.
49. Kataoka Y, Wolski K, Uno K, et al. Spotty calcification as a marker of accelerated progression of coronary atherosclerosis: insights from serial intravascular ultrasound. *J Am Coll Cardiol* 2012;59:1592-7.
50. Dussaillant GD, Mintz GS, Pichard AD, et al. Intravascular ultrasound identification of calcified intraluminal lesions misdiagnosed as thrombi by coronary angiography. *Am Heart J* 1996;132:687-9.
51. Lee JB, Mintz GS, Lissauskas JB, et al. Histopathologic validation of the intravascular ultrasound diagnosis of calcified coronary artery nodules. *Am J Cardiol* 2011;108:1547-51.
52. Jia H, Abtahian F, Aguirre AD, et al. In vivo diagnosis of plaque erosion and calcified nodule in patients with acute coronary syndrome by intravascular optical coherence tomography. *J Am Coll Cardiol* 2013;62:1748-58.
53. Xu Y, Mintz GS, Tam A, et al. Prevalence, distribution, predictors, and outcomes of patients with calcified nodules in native coronary arteries: a 3-vessel intravascular ultrasound analysis from Providing Regional Observations to Study Predictors of Events in the Coronary Tree (PROSPECT). *Circulation* 2012;126:537-45.
54. Hong MK, Mintz GS, Lee CW, et al. The site of plaque rupture in native coronary arteries: a three-vessel intravascular ultrasound analysis. *J Am Coll Cardiol* 2005;46:261-5.
55. Wykrzykowska JJ, Mintz GS, Garcia-Garcia HM, et al. Longitudinal distribution of plaque burden and necrotic core-rich plaques in nonculprit lesions of patients presenting with acute coronary syndromes. *J Am Coll Cardiol* 2012;59:510-8.
56. Fujii K, Kawasaki D, Masutani M, et al. OCT assessment of thin-cap fibroatheroma distribution in native coronary arteries. *J Am Coll Cardiol* 2010;3:168-75.
57. Wang JC, Normand SL, Mauri L, Kuntz RE. Coronary artery spatial distribution of acute myocardial infarction occlusions. *Circulation* 2004;110:278-84.
58. Cheruvu PK, Finn AV, Gardner C, et al. Frequency and distribution of thin-cap fibroatheroma and ruptured plaques in human coronary arteries: a pathologic study. *J Am Coll Cardiol* 2007;50:940-9.
59. Kelly-Arnold A, Maldonado N, Laudier D, Aikawa E, Cardoso L, Weinbaum S. Revised microcalcification hypothesis for fibrous cap rupture in human coronary arteries. *Proc Natl Acad Sci U S A* 2013;110:10741-6.
60. Cardoso L, Kelly-Arnold A, Maldonado N, Laudier D, Weinbaum S. Effect of tissue properties, shape and orientation of microcalcifications on vulnerable cap stability using different hyperelastic constitutive models. *J Biomech* 2014;47:870-7.
61. Virmani R, Burke AP, Kolodgie FD, Farb A. Pathology of the thin-cap fibroatheroma: a type of vulnerable plaque. *J Interv Cardiol* 2003;16:267-72.
62. Liu L, Gardecki JA, Nadkarni SK, et al. Imaging the subcellular structure of human coronary atherosclerosis using micro-optical coherence tomography. *Nat Med* 2011;17:1010-4.
63. Mintz GS. Clinical utility of intravascular imaging and physiology in coronary artery disease. *J Am Coll Cardiol* 2014;64:207-22.
64. Latib A, Takagi K, Chizzola G, et al. Excimer laser lesion modification to expand non-dilatable stents: the ELLEMENT registry. *Cardiovasc Revasc Med* 2014;15:8-12.
65. Hoffmann R, Mintz GS, Popma JJ, et al. Treatment of calcified coronary lesions with Palmaz-Schatz stents. An intravascular ultrasound study. *Eur Heart J* 1998;19:1224-31.
66. Henneke KH, Regar E, König A, et al. Impact of target lesion calcification on coronary stent expansion after rotational atherectomy. *Am Heart J* 1999;137:93-9.
67. Tang Z, Bai J, Su SP, et al. Cutting-balloon angioplasty before drug-eluting stent implantation for the treatment of severely calcified coronary lesions. *J Geriatr Cardiol* 2014;11:44-9.
68. Kobayashi Y, Okura H, Kume T, et al. Impact of target lesion coronary calcification on stent expansion. *Circ J* 2014;78:2209-14.
69. Vavuranakis M, Toutouzas K, Stefanadis C, Chrisohou C, Markou D, Toutouzas P. Stent deployment in calcified lesions: can we overcome calcific restraint with high-pressure balloon inflations? *Catheter Cardiovasc Interv* 2001;52:164-72.
70. Mintz GS, Kovach JA, Javier SP, et al. Mechanisms of lumen enlargement after excimer laser coronary angioplasty. An intravascular ultrasound study. *Circulation* 1995;92:3408-14.
71. Rawlins J, Talwar S, Green M, O'Kane P. Optical coherence tomography following percutaneous coronary intervention with Excimer laser coronary atherectomy. *Cardiovasc Revasc Med* 2014;15:29-34.
72. Kovach JA, Mintz GS, Pichard AD, et al. Sequential intravascular ultrasound characterization of the mechanisms of rotational atherectomy and adjunct balloon angioplasty. *J Am Coll Cardiol* 1993;22:1024-32.
73. Attizzani GF, Patrício L, Bezerra HG. Optical coherence tomography assessment of calcified plaque modification after rotational atherectomy. *Catheter Cardiovasc Interv* 2013;81:558-61.
74. von Birgelen C, Mintz GS, Böse D, et al. Impact of moderate lesion calcium on mechanisms of coronary stenting as assessed with three-dimensional intravascular ultrasound in vivo. *Am J Cardiol* 2003;92:5-10.

75. Sato K, Naganuma T, Costopoulos C, et al. Calcification analysis by intravascular ultrasound to define a predictor of left circumflex narrowing after cross-over stenting for unprotected left main bifurcation lesions. *Cardiovasc Revasc Med* 2014; 15:80-5.
76. Mehran R, Dangas G, Mintz GS, et al. Atherosclerotic plaque burden and CK-MB enzyme elevation after coronary interventions: intravascular ultrasound study of 2256 patients. *Circulation* 2000;101:604-10.
77. Mosseri M, Satler LF, Pichard AD, Waksman R. Impact of vessel calcification on outcomes after coronary stenting. *Cardiovasc Revasc Med* 2005; 6:147-53.
78. Ueda T, Uemura S, Watanabe M, et al. Colocalization of thin-cap fibroatheroma and spotty calcification is a powerful predictor of procedure-related myocardial injury after elective coronary stent implantation. *Coron Artery Dis* 2014;25: 384-91.
79. Patel VG, Brayton KM, Mintz GS, Maehara A, Banerjee S, Brilakis ES. Intracoronary and noninvasive imaging for prediction of distal embolization and periprocedural myocardial infarction during native coronary artery percutaneous intervention. *Circ Cardiovasc Imaging* 2013;6: 1102-14.
80. Kim SW, Mintz GS, Ohlmann P, et al. Frequency and severity of plaque prolapse within Cypher and Taxus stents as determined by sequential intravascular ultrasound analysis. *Am J Cardiol* 2006;98:1206-11.
81. Potkin BN, Keren G, Mintz GS, et al. Arterial responses to balloon coronary angioplasty: an intravascular ultrasound study. *J Am Coll Cardiol* 1992;20:942-51.
82. Fitzgerald PJ, Ports TA, Yock PG. Contribution of localized calcium deposits to dissection after angioplasty. An observational study using intravascular ultrasound. *Circulation* 1992;86:64-70.
83. Liu X, Tsujita K, Maehara A, et al. Intravascular ultrasound assessment of the incidence and predictors of edge dissections after drug-eluting stent implantation. *J Am Coll Cardiol Intv* 2009; 2:997-1004.
84. Maehara A, Mintz GS, Bui AB, et al. Incidence, morphology, angiographic findings, and outcomes of intramural hematomas after percutaneous coronary interventions: an intravascular ultrasound study. *Circulation* 2002;105:2037-42.
85. Lindsay AC, Paulo M, Kadriye K, et al. Predictors of stent strut malapposition in calcified vessels using frequency-domain optical coherence tomography. *J Invasive Cardiol* 2013;25:429-34.
86. Morlacchi S, Pennati G, Petrini L, Dubini G, Migliavacca F. Influence of plaque calcifications on coronary stent fracture: a numerical fatigue life analysis including cardiac wall movement. *J Biomech* 2014;47:899-907.
87. Shimada Y, Kataoka T, Courtney BK, et al. Influence of plaque calcium on neointimal hyperplasia following bare metal and drug-eluting stent implantation. *Catheter Cardiovasc Interv* 2006;67: 866-9.
88. Kaneda H, Koizumi T, Ako J, et al. Impact of intravascular ultrasound lesion characteristics on neointimal hyperplasia following sirolimus-eluting stent implantation. *Am J Cardiol* 2005;96: 1237-41.
89. Puri R, Libby P, Nissen SE, et al. Long-term effects of maximally intensive statin therapy on changes in coronary atheroma composition: insights from SATURN. *Eur Heart J Cardiovasc Imaging* 2014;15:380-8.
90. Zhao Z, Witzensbichler B, Mintz GS, et al. Dynamic nature of nonculprit coronary artery lesion morphology in STEMI: a serial IVUS analysis from the HORIZONS-AMI trial. *J Am Coll Cardiol Img* 2013;6:86-95.
91. Kubo T, Maehara A, Mintz GS, et al. The dynamic nature of coronary artery lesion morphology assessed by serial virtual histology intravascular ultrasound tissue characterization. *J Am Coll Cardiol* 2010;55:1590-7.
92. Dohi T, Mintz GS, McPherson JA, et al. Non-fibroatheroma lesion phenotype and long-term clinical outcomes: a substudy analysis from the PROSPECT study. *J Am Coll Cardiol Img* 2013;6: 908-16.
93. Kubo T, Ino Y, Tanimoto T, Kitabata H, Tanaka A, Akasaka T. Optical coherence tomography imaging in acute coronary syndromes. *Cardiol Res Pract* 2011;2011:312978.

KEY WORDS calcium, intravascular ultrasound, optical coherence tomography